Bioresource Technology 353 (2022) 127141

Contents lists available at ScienceDirect

Bioresource Technology

journal homepage: www.elsevier.com/locate/biortech

Production of (*R*)-3-hydroxybutyric acid from methane by *in vivo* depolymerization of polyhydroxybutyrate in *Methylocystis parvus* OBBP

Luz Yáñez [a,b], Yadira Rodríguez [a], Felipe Scott [b], Alberto Vergara-Fernández [b], Raúl Muñoz [a,*]

[a] Institute of Sustainable Processes, Universidad de Valladolid, Doctor Mergelina s/n, 47011, Spain
[b] Green Technology Research Group, Facultad de Ingeniería y Ciencias Aplicadas, Universidad de Los Andes, 7550000, Chile

HIGHLIGHTS

- PHB accumulated in *M. parvus* was depolymerized under alkaline conditions.
- The depolymerization produced (R)-3-hydroxybutyrate with a 77% conversion.
- The presence of a nitrogen source promoted depolymerization and monomer release.
- Low O_2 supply rates and high monomers concentration reduced PHB depolymerization.

GRAPHICAL ABSTRACT

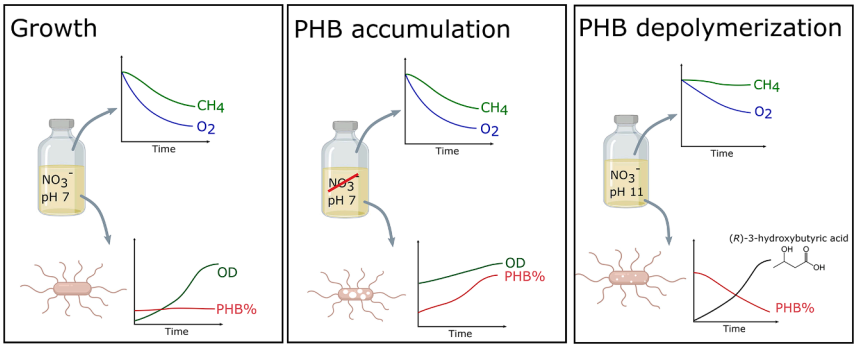

ARTICLE INFO

Keywords:
(*R*)-3-hydroxybutyrate
Chiral compounds
Greenhouse gas valorization
Methanotrophic bacteria
Polyhydroxybutyrate

ABSTRACT

Methylocystis parvus OBBP accumulates polyhydroxybutyrate (PHB) using methane as the sole carbon and energy source. In this work, the feasibility of producing (*R*)-3-hydroxybutyric acid (R3HBA) via intracellularly accumulated PHB through depolymerization (*in-vivo)* was investigated. Results showed that a PHB to R3HBA conversion of 77.2 ± 0.9% (R3HBA titer of 0.153 ± 0.002 g L^{-1}) can be attained in a mineral medium containing 1 g L^{-1} KNO_3 at 30 °C with shaking at 200 rpm and a constant pH of 11 for 72 h. Nitrogen deprivation and neutral or acidic pHs strongly reduced the excreted R3HBA concentration. Reduced oxygen availability negatively affected the R3HBA yield, which decreased to 73.6 ± 4.9% (titer of 0.139 ± 0.01 g L^{-1}) under microaerobic conditions. Likewise, the presence of increasing concentrations of R3HBA in the medium before the onset of PHB depolymerization reduced the initial R3HBA release rate and R3HBA yield.

1. Introduction

Methane (CH_4) is an inexpensive, colorless, odorless, and abundant gas that represents a widely available carbon and energy source. In 2019, CH_4 accounted for nearly 10 % of all U.S. anthropogenic greenhouse gas emissions (Jackson et al., 2020). The largest CH_4 sources included anthropogenic emissions from agriculture, waste and the extraction and use of fossil fuels (Kirschke et al., 2013; Saunois et al.,

* Corresponding author.
E-mail addresses: lfyanez@miuandes.cl (L. Yáñez), yadira.rodriguez@uva.es (Y. Rodríguez), fscott@miuandes.cl (F. Scott), aovergara@miuandes.cl (A. Vergara-Fernández), mutora@iq.uva.es (R. Muñoz).

https://doi.org/10.1016/j.biortech.2022.127141
Received 9 March 2022; Received in revised form 6 April 2022; Accepted 7 April 2022
Available online 9 April 2022

2016). The Global Methane Assessment report shows that decreasing methane emission by 45% during this decade would avoid 0.3 °C of global warning by 2045. Moreover, nearly a quarter-million premature deaths and 25 million tons of crop losses could be prevented annually (Ravishankara et al., 2021). CH_4 emissions contribute to almost one-quarter of the cumulative radiative forcing of carbon dioxide (CO_2), CH_4 and nitrous oxide (N_2O) combined since 1750 (Etminan et al., 2016). Although the lifetime of CH_4 in the atmosphere is much shorter than that of CO_2, it absorbs thermal infrared radiation much more efficiently. Indeed, CH_4 exhibits a global warming potential 86 times stronger per unit of mass than CO_2 on a 20-year timescale and approximately 28 times more powerful on a 100-year time scale (Edenhofer, 2014). Today, CH_4 can be captured from landfills (38 Mt/year), wastewater treatment (21 Mt/year), agriculture (11–30 Mt/year), biomass (10 Mt/year), and natural gas production (92 Mt/year) (Strong et al., 2015). This methane can be valorized as an energy vector or as a feedstock for the biological production of products such as ectoine, biopolymers, and single cell proteins, among others (Jawaharraj et al., 2020) or for the catalytic production of methanol (Latimer et al., 2018). In this context, CH_4 represents a carbon and energy source for a group of gram-negative bacteria known as methanotrophs. These bacteria are classified according to the pathways used for the assimilation of the formaldehyde directly derived from CH_4 into type I and type II methanotrophs. Type I using the ribulose monophosphate pathway for formaldehyde assimilation, and type II methanotrophs using the serine pathway (Nguyen et al., 2021). *Methylocystis parvus* is a type II methanotroph that shows a higher specific growth rate compared to other species of the *Methylocystis* genera (Bordel et al., 2019) and the ability to synthesize the biopolymer polyhydroxybutyrate (PHB) under nitrogen-limited conditions (Rostkowski et al., 2013). *M. parvus* has been reported to accumulate more than 50% (Pieja et al., 2011; Wendlandt et al., 2001) of its dry weight as PHB, which renders it a suitable industrial biopolymer producer.

In *M. parvus,* PHB synthesis starts with the condensation of two acetyl-CoA molecules, see Fig. 2A (Bordel et al., 2019). This pathway is conserved in many bacteria such as *Ralstonia eutropha*, *Azohydromonas* spp., *Azotobacter* spp., among others (McAdam et al., 2020), where acetyl-CoA molecules can be supplied from a wide range of carbon sources. These include simple sugars and organic acids (Sirohi et al., 2020), food residues, and industrial by-products (Liu et al., 2021). Bacteria rely on PHB depolymerases (PhaZ), located intracellularly, to catabolize this stored reserve of carbon and energy (Müller-Santos et al., 2021), yielding the monomer (*R*)-3-hydroxybutyric acid (R3HBA) and dimers (Jendrossek and Handrick, 2002). If conditions are permissive for growth, the released R3HBA will act as a source of carbon and energy (Donoso et al., 2011), starting with the conversion of R3HBA to acetoacetate by the NADH-dependent enzyme (*R*)-3-hydroxybutyrate dehydrogenase (Bdh) (Tokiwa and Ugwu, 2007). If environmental conditions do not support growth, or part of the R3HBA consumption pathway is blocked, the monomer is excreted to the media (Lee et al., 1999). This strategy has been implemented in non-methanotrophic PHB producers to obtain R3HBA in the cultivation broth during PHB depolymerization. While for *Azohydromonas lata* a pH of 4.0 produced the highest titer and yield of R3HBA, a pH of 9.2 was required for the liberation of hydroxyalkanoic acids from polyhydroxyalkanoates in *Pseudomonas putida* (Ruth et al., 2007).

R3HBA is a chiral molecule that can be applied as a building block in the synthesis of fine chemicals and pharmaceutical products such as biopolymers, antibiotics (Ren et al., 2005), insecticides and fragrances (Matsuyama et al., 2001; Yañez et al., 2020). R3HBA and its derivatives have been also used as potential drugs. For example, the infusion of 3RHBA improved ATP production in mitochondria and confers partial protection against neurodegenerative disease in a Parkinson mice model (Tieu et al., 2003). Outcomes of depression (Yamanashi et al., 2017), osteoporosis (Cao et al., 2014), Alzheimer (Zhang et al., 2013), and cardiovascular diseases (Nielsen et al., 2019) have been shown to improve using a 3HBA infusion. As a dietary supplement, the price of 3HBA is within 130–160 USD/kg (Fruggo," 2021). However, the conventional synthesis, extraction and purification of R3HBA from PHB produced from sugar-based bacterial processes is nowadays expensive (Pérez-Rivero et al., 2019), which requires alternative PHB production pathways with streamlined downstream processes in order to enhance process economics.

This work aims at determining the environmental conditions (presence or absence of carbon and nitrogen sources, pH, temperature) that lead to the production of R3HBA in the culture supernatant using the native PHB depolymerization pathway in *M. parvus*. The underlying hypothesis is that a combination of these variables would result in an active PHB depolymerase and an inactive or inhibited (*R*)-3-hydroxybutyrate dehydrogenase, as previously shown for other gram negative bacteria (Lee et al., 1999; Ren et al., 2005, 2007; Ruth et al., 2007).

2. Materials and methods

2.1. Mineral salt medium

Nitrate mineral salt (NMS) medium (pH 6.8) was composed of (g L^{-1}): 1.0 KNO_3, 1.1 $MgSO_4{\cdot}7H_2O$, 0.8 $Na_2HPO_4{\cdot}12H_2O$, 0.26 KH_2PO_4 and 0.2 $CaCl_2{\cdot}2H_2O$; and 1 mL of trace element solution (g L^{-1}): 0.3 $Na_2MoO_4{\cdot}2H_2O$, 0.3 $Na_2EDTA{\cdot}2H_2O$, 1 $CuSO_4{\cdot}5H_2O$, 0.5 $FeSO_4{\cdot}7H_2O$, 0.4 $ZnSO_4{\cdot}7H_2O$, 0.03 $CoCl_2$, 0.02 $MnCl_2{\cdot}4H_2O$, 0.015 H_3BO_3, 0.01 $NiCl_2{\cdot}6H_2O$ and 0.38 Fe-EDTA. Nitrate-free mineral salt (NFMS) medium was identical to NMS medium except that potassium nitrate was omitted. The reagents were acquired from PanReac AppliChem (Spain), except KNO_3, which was purchased from COFARCAS (Spain).

2.2. Inocula preparation

The methanotrophic strain *Methylocystis parvus* OBBP, kindly provided by Biopolis S.L. (Valencia, Spain), was inoculated (10% v/v) under sterile conditions in 125-mL crimp-sealed serum bottles containing 50 mL of (NMS) medium. The headspace (75 mL) of the bottles was flushed under sterile conditions for 5 min with filtered oxygen (0.22 μm, Millex GP, Merck). Then, 25 mL of the oxygen headspace atmosphere was replaced with sterile methane, resulting in an O_2:CH_4 concentration ratio of 66.7:33.3% (v/v). The cultures were incubated at 30 °C and 230 rpm in an orbital shaker (MaxQ 4000; Thermo Scientific, USA) for 5 days, unless otherwise stated. The headspace atmosphere of the bottles was replaced 6 times upon CH_4 depletion.

Then, biomass was collected and transferred into 2.2 L serum bottles containing 0.4 L of NMS, crimp sealed under a O_2:CH_4 atmosphere of 66.7%:33.3% until complete methane depletion (~10 days). The headspace atmosphere was obtained by flushing for 3 min a gas mixture as described above from a 100 L-Tedlar gas sampling bag (Sigma-Aldrich, USA). The cultures were grown at 25 °C (thermostated room) with an initial pH of 6.9 and magnetically stirred at 300 rpm (Poly 15 Variomag, Thermo Fisher Scientific).

When methane was depleted, the biomass was collected by centrifugation at 10000 rpm for 8 min (Sorvall Legend RT+; Thermo Scientific, USA) and re-suspended into 0.4 L of NFMS medium to promote PHB accumulation for ~ 10 days under similar incubation conditions.

2.3. Optimization of PHB depolymerization in M. Parvus

Unless otherwise indicated, the experiments were performed batch wise using PHB containing biomass in 125 mL serum bottles (working volume of 45 mL) crimp sealed (three biological replicates). The bottles were incubated at 30 °C (except Test 3) and 230 rpm in an orbital shaker.

2.3.1. Test 1. Influence of the presence of nitrate and O_2, and pH on PHB depolymerization

The assays were performed with NMS and NFMS media at both pH 4 and pH 11 in triplicate for 48 h. All cultures were inoculated with 10 mL of concentrated *M. parvus* culture previously grown in NFMS for 10 days (1.3 gTSS L^{-1} with 51,4% of PHB) and were incubated for two days under an O_2:CH_4 headspace (66.7%:33.3%) and a He:CH_4 atmosphere (66.7%:33.3%). A control test at pH 7 under a O_2:CH_4 headspace (66.7%:33.3%) and NMS media was also carried out. Culture samples were collected periodically for the quantification of the R3HBA concentration. Total suspended solids (TSS), total nitrogen, PHAs, and pH were determined at the beginning and end of the experiment.

2.3.2. Test 2. Optimization of pH during PHB depolymerization

PHB depolymerization under an O_2:CH_4 atmosphere (66.7%:33.3%) was assessed in triplicate at pH 10, pH 11 and pH 12 with NMS medium as above described for 48 h. The pH of the cultures was monitored three times per day and manually adjusted using 5 M NaOH, while the concentration of extracellular R3HBA was quantified once per day. The biomass concentration (estimated as TSS) and PHB cells content were determined at the beginning and the end of the experiment.

2.3.3. Test 3. Influence of temperature on the kinetic of PHB depolymerization

PHB depolymerization at pH 11 on NMS medium was assessed in triplicate at 25 and 35 °C for 3 h using fresh *M. parvus* with a concentration and PHB cell content of 4.17 gTSS L^{-1} and 44.7%. The determination of extracellular R3HBA concentration was conducted at 15, 30, 60, 120 and 180 min. At the end of the experiment, cell viability was evaluated using the pellets obtained after centrifugation of the biomass from depolymerized cells. Cell viability tests were performed at 25 °C in 2.2 L serum bottles with a working volume of 0.4 L of both NMS and NFMS medium. The bottles were capped with aluminum caps and chlorobutyl rubber stoppers under and O_2:CH_4 atmosphere (66.7:33.3%) and incubated as above described (section 2.2) until complete CH_4 depletion. TSS, CH_4, O_2 and CO_2 concentrations were periodically measured.

2.3.4. Test 4. Influence of the initial R3HBA concentration and aeration rate on PHB depolymerization

The influence of the oxygen mass transfer rate on PHB depolymerization and R3HBA yield was investigated in Erlenmeyer flasks (E-flasks) incubated at 200 rpm and 30 °C in an orbital shaker for 72 h. The lowest oxygen mass transfer rate was achieved in 100 mL E-flasks containing 100 mL of medium, while the highest oxygen transfer rate was reached in 250 mL E-flasks containing 50 mL of cultivation broth. An intermediate condition was tested in 100 mL E-flasks containing 50 mL of cultivation broth. The initial biomass concentration and PHB content of the cell suspension was 0.51 ± 0.005 gTSS L^{-1} and 31.9 ± 1.88% PHB, respectively. The experiments were conducted in duplicate.

The potential inhibitory effect of extracellular R3HBA over PHB depolymerization was investigated using R3HBA produced *in-house* following the procedure described by Lee et al. (1999). Briefly, *Azohydromonas lata* (DSM 1123, Leibniz Institute, Germany) was cultivated from a frozen stock culture in a nutrient agar plate. A single colony was picked and used to inoculate a 500 mL E-flask with 100 mL of AL1 medium (Wang and Lee, 1997). This culture served as the inoculum for a batch bioreactor cultivation of this bacterium in a Labfors 5 bioreactor (Infors HT, Switzerland). The bioreactor was operated with 1 L of AL2 medium containing an initial glucose concentration of 30 g L^{-1} and an initial ammonium sulfate concentration of 2 g L^{-1}. Dissolved oxygen was maintained above 40% saturation by varying the stirring speed up to 700 rpm at 1 vvm air. When necessary, pure oxygen was automatically mixed with the inlet air flow under a cascade control. After 24 h of cultivation, approximately 12.0 g L^{-1} of biomass were retrieved containing a PHB cell content of 75%. Cells were collected by centrifugation, washed twice with distilled water, and resuspended in water at a concentration of approximately 120 gTSS L^{-1}. PHB depolymerization was started by adjusting the pH to 4.0 with HCl and lasted for 1 h. The pH was controlled at 4.0 using 2 M NaOH. Following the purification procedure outlined in Lee et al. (1999), a solution containing 34.2 g L^{-1} of sodium (*R*)-3-hydroxybutyrate was obtained. HPLC analysis indicated that the solution contained trace levels of other unidentified compounds and crotonic acid. Finally, *M. parvus* cells containing PHB were washed and resuspended in NMS medium at pH 11 supplemented with R3HBA at concentrations of 0, 120, 330 and 650 mg L^{-1}. Cell incubation was performed in 100 mL E-flasks containing 50 mL of cell suspension with the corresponding R3HBA concentration at 30 °C and 200 rpm in an orbital shaker.

Culture samples were collected at 0, 3, 6, 48 and 72 h for R3HBA and crotonic acid quantification. The biomass and PHB cell content were monitored at the beginning and the end of experiments.

2.4. PHB depolymerization and R3HBA yields calculation

The PHB depolymerization percentage conversion (%) was calculated according to Eq. (1):

$$C_{PHB} = 100 \times \frac{X^i_{PHB} - X^f_{PHB}}{X^i_{PHB}} \quad (1)$$

The R3HBA molar yield was calculated as the ratio of the moles of R3HBA excreted and the moles of PHB consumed, considering that PHB hydrolysis consumes one mol of water per mol of R3HBA produced (Eq. (2)):

$$Y_{R3HBA} = 100\left(\frac{104.10 - 18.01}{104.10}\right)\frac{X^f_{R3HBA} - X^i_{R3HBA}}{X^i_{PHB} - X^f_{PHB}} \quad (2)$$

where X^i_{PHB} and X^f_{PHB} correspond to the initial and final PHB concentrations (g L^{-1}), and X^i_{3HBA} and X^f_{3HBA} represent the initial and final concentrations of R3HBA (g L^{-1}). A similar calculation was used for the crotonic acid yield (Y_{crot}). The conversion of PHB to R3HBA can be calculated as the product $0.01 \cdot Y_{R3HBA} \cdot C_{PHB}$.

Finally, the specific R3HBA release rate per gram of initial intracellular PHB (q_{R3HBA}) was calculated as follows.

$$q_{R3HBA} = \frac{m}{X^i_{PHB}} \quad (3)$$

Where *m* is the slope of the line whose independent and dependent variables are the depolymerization time and R3HBA concentration (in mg L^{-1}), respectively.

2.5. Analytical procedures

CH_4, CO_2 and O_2 gas concentrations were measured in gas a chromatograph coupled with a thermal conductivity detector (Bruker 430 GC-TCD, Bruker Corporation, USA) following the method described by Estrada et al. (2014). The optical density of the cultures samples was measured by spectrophotometry at 600 nm (UV-2550, Shimadzu, Japan). TSS and pH were analyzed according to Rodríguez et al. (2020). PHB was quantified via gas chromatography-mass spectrometry (GC–MS) (Rodríguez et al., 2020) or GC-FID (Scott et al., 2021). The concentration of R3HBA was determined using a commercial (*R*)-3-Hydroxybutyric Acid Assay Kit (Megazyme, Ireland) according to manufacturer's protocol or using HPLC with a UV–Vis detector at 210 nm and a refractive index detector (Prominence, Shimadzu) according to Scott et al. (2021). Citrate, succinate, malate and crotonic acids (Sigma-Aldrich catalog number, 113018) were quantified using the HPLC-UV-IR method described by Scott et al. (2021). The organic acids standard was purchased from Biorad (catalog number, 125–0586).

3. Results and discussion

3.1. Influence of the presence of nitrate and O_2, and pH on PHB depolymerization

Fig. 1 shows the methane and oxygen consumption for the 48 h depolymerization experiments performed with NMS (Fig. 1A and B) and NFMS (Fig. 1C and D) at pH 4, 7 and 11. Consumption of methane and oxygen was faster in the control experiment with NMS at pH 7 compared to that in NFMS medium, an expected result considering that NMS allows for balanced growth. In the absence of oxygen at pH 7, methane consumption was negligible in NFMS medium and close to 10% in the NMS cultures. In this regard, Bordel et al., (2019) showed that *M. parvus* can use stored PHB as an energy source under anoxic conditions only when nitrate is available in the cultivation broth. The annotated genome of *M. parvus* contains the genes involved in nitrate reduction and revealed that denitrification is the only mechanism supporting the use of methane or PHB as an energy source in the absence of oxygen (Bordel et al., 2019).

Both pHs of 11 and 4 induced an important reduction in the consumption of methane and oxygen compared to the control tests. Thus, methane consumption was negligible at pH 11 in NMS medium, while the final consumption of oxygen accounted for 64.8 ± 9.54% of the initial O_2 present in the headspace (compared to 87.8 ± 0.82% of the control), suggesting the occurrence of a respiratory metabolism fueled by a substrate different than methane. pH 4 supported an oxygen and methane final consumption of 33.4 ± 12.67 and 30.6 ± 14.14%, respectively. On the other hand, neither methane nor oxygen consumption was recorded at pH 4 in NFMS medium. Similarly, at pH 11 the final consumption of CH_4 (37.41 ± 6.81%) and the O_2 uptake (30.14 ± 4.65) were reduced compared to the control.

In NMS, nitrate was consumed only in the control assays at pH 7 from the initial 130.1 mgN L^{-1} (measured as total nitrogen) to 47.8 ± 11.5 mgN L^{-1} at the end of the 48 h incubation period. Nitrate consumption at pHs 4.0 and 11.0 was lower than 2.6 mgN L^{-1} during the same period, and only 0.3 mgN L^{-1} was consumed in the assay at pH 7 in the absence of oxygen. Therefore, no significant cell growth occurred except in the control assay at neutral pH.

Interestingly, extracellular R3HBA was only detected at pH 11 in both NMS and NFMS medium (Fig. 1E). At pH 11 in NMS, 80.6 ± 0.8% of PHB was depolymerized and R3HBA secretion reached 205.8 ± 1.2 mg L^{-1}, a higher concentration compared with the assay in NFMS, where 25.7 ± 7.9% of PHB was depolymerized and a R3HBA titer of 60.1 ± 12.9 mg L^{-1} was measured after 48 h. The mechanisms by which nitrogen influences the depolymerization extent and rate seem to be related to the alleviation of the stringent response. In amino acid starved cells, the alarmone ppGpp accumulates and destabilizes the RNA polymerase σ^{70}, resulting in an induction of genes under the control of alternative sigma σ factors, such as σ^{54} (Brigham et al., 2012). ppGpp has also been implicated in the inhibition of translation (Irving et al., 2021). In *Ralstonia eutropha* H16, PHB mobilization occurs in the absence of the alarmone ppGpp, which in turn requires the presence of a source of nitrogen (Juengert et al., 2017). As further evidence of this mechanism, the genome of *M. parvus* OBBP contains the necessary bifunctional (p)ppGpp synthetase/hydrolase (WP_016921527.1) required for the synthesis and degradation of ppGpp.

PHB depolymerization at pH 4 and pH 7 (with or without O_2) in NMS supported extracellular R3HBA concentrations of 5.42 ± 0.67 mg L^{-1}, 4.83 ± 0.37 mg L^{-1} and 4.01 ± 0.15 mg L^{-1}, respectively. Similarly, extracellular R3HBA concentrations of 4.68 ± 0.37 mg L^{-1}, 6.17 ± 0.22

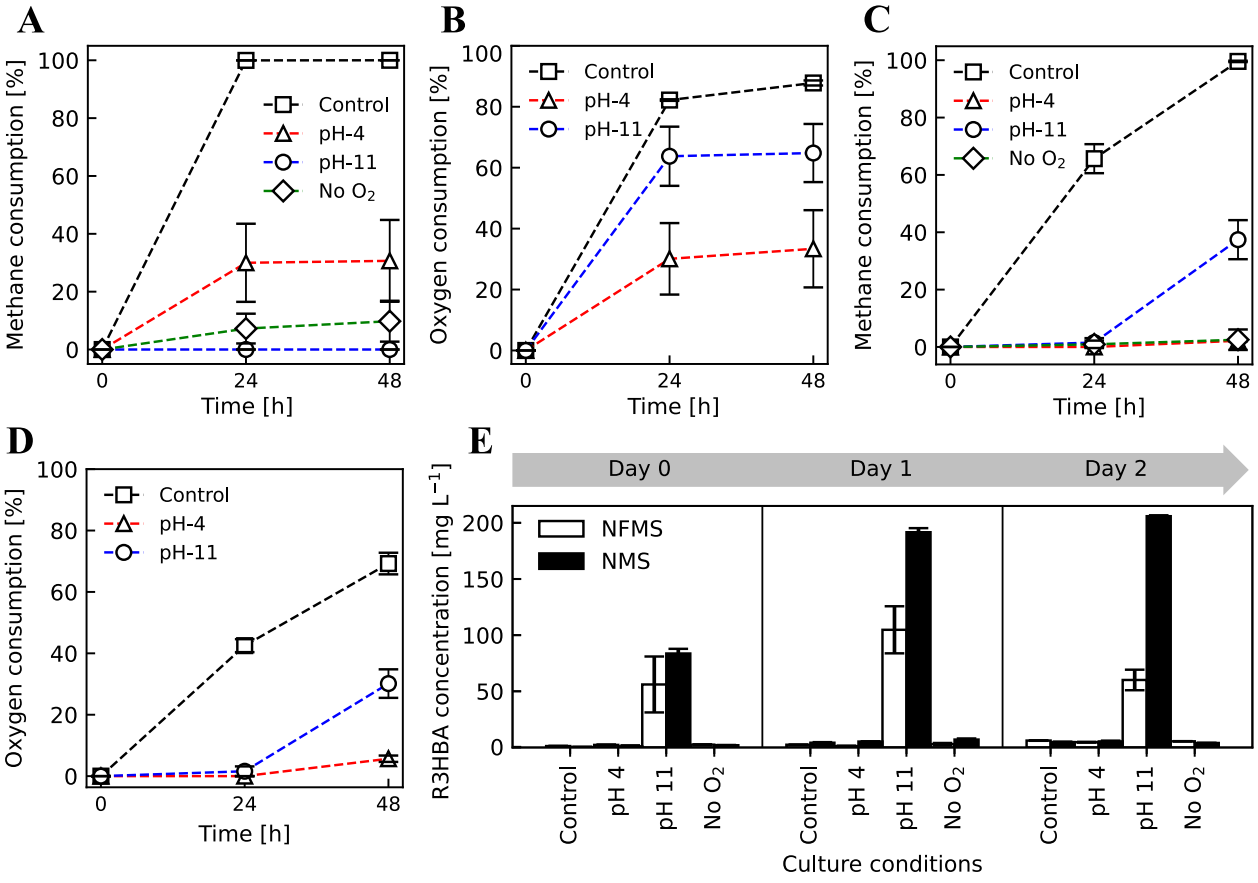

Fig. 1. CH_4 and O_2 consumption during PHB depolymerization in *M. parvus* cultivated in NMS (A, B) and NFMS (C, D) medium at pH 4 (triangles), pH 11 (circles), pH 7 (squares) and without oxygen at pH 7 (diamonds). (E) R3HBA released in *M. parvus* cultures at pH 4, pH 11, pH 7 (with and without oxygen) in NMS (black bars) and NFMS (white bars) medium.

mg L^{-1} and 5.50 ± 0.15 mg L^{-1} were measured after 48 h in NFMS at pH 4 and pH 7 with or without oxygen, respectively. The final pH of the culture broth in the assays initially adjusted to pH 11 in NMS and NFMS media decreased to 8.28 and 6.23, respectively, confirming the secretion of the acidic R3HBA. No significant changes in pH were measured in the rest of the experiments, which agreed with the limited R3HBA release. The estimated Y_{R3HBA} are 31.5 ± 0.08% and 28.9 ± 0.91%, which equates to a PHB to R3HBA conversion of 25.4 ± 0.03% and 7.4 ± 2.1%, for the experiments at initial pH of 11 in NMS and NFMS, respectively.

The *in-vivo* depolymerization of the intracellularly accumulated PHAs to hydroxy acids has been reported in several bacterial strains. For instance, the depolymerization process in *Azohydromonas lata* was carried out in water without shaking to minimize oxygen transfer, at 37 °C and pH 4.0, and achieved a depolymerization efficiency of 96% of the initial PHB to R3HBA in only 30 min (Lee et al., 1999). These author also evaluated PHB depolymerization in *Pseudomonas aeruginosa* PAO1 (DSM 1707), *Pseudomonas oleovorans* (ATCC 29347) and *Cupriavidus necator* (NCIMB 11599) at pH values below 7.0 (Lee et al., 1999). The PHA to hydroxyacids conversion was 20% for *C. necator* and less than 10% for *Pseudomonas* species (Lee et al., 1999).

The conversion of PHA to hydroxyacids in *Pseudomonas putida* GPo1 was improved by changing the depolymerization conditions to an alkaline medium. This strain excreted (*R*)-3-hydroxyoctanaoic (R3HO) acid and (*R*)- 3-hydroxyhexanoic acid (R3HHx) at pH 11 in citrate buffer for 6 h with a PHA degradation efficiency and monomer production yields above 90% (w/w) (Ren et al., 2005). Ruth et al., (2007) engineered a depolymerization strategy at pH 10 in *P. putida* GPo1 under continuous mode with a production of R3HO, R3HHx, (*R*)-3-hydroxy-10 undecenoic acid, (*R*)-3-hydroxy-8-nonenoic acid, (*R*)-3-hydroxy-6-heptenoic acid, (*R*)-3hydroxyundecanoic acid, (*R*)-3-hydroxynonanoic acid, and (*R*)-3 hydroxyheptanoic acid. The study herein presented confirmed the key role of high pH on PHA depolymerization, which is a common feature in *Pseudomonas* species. Hence, *P. putida* GPo1 released 3-hydroxyoctanoic acid and 3-hydroxyhexanoic acid from intracellular

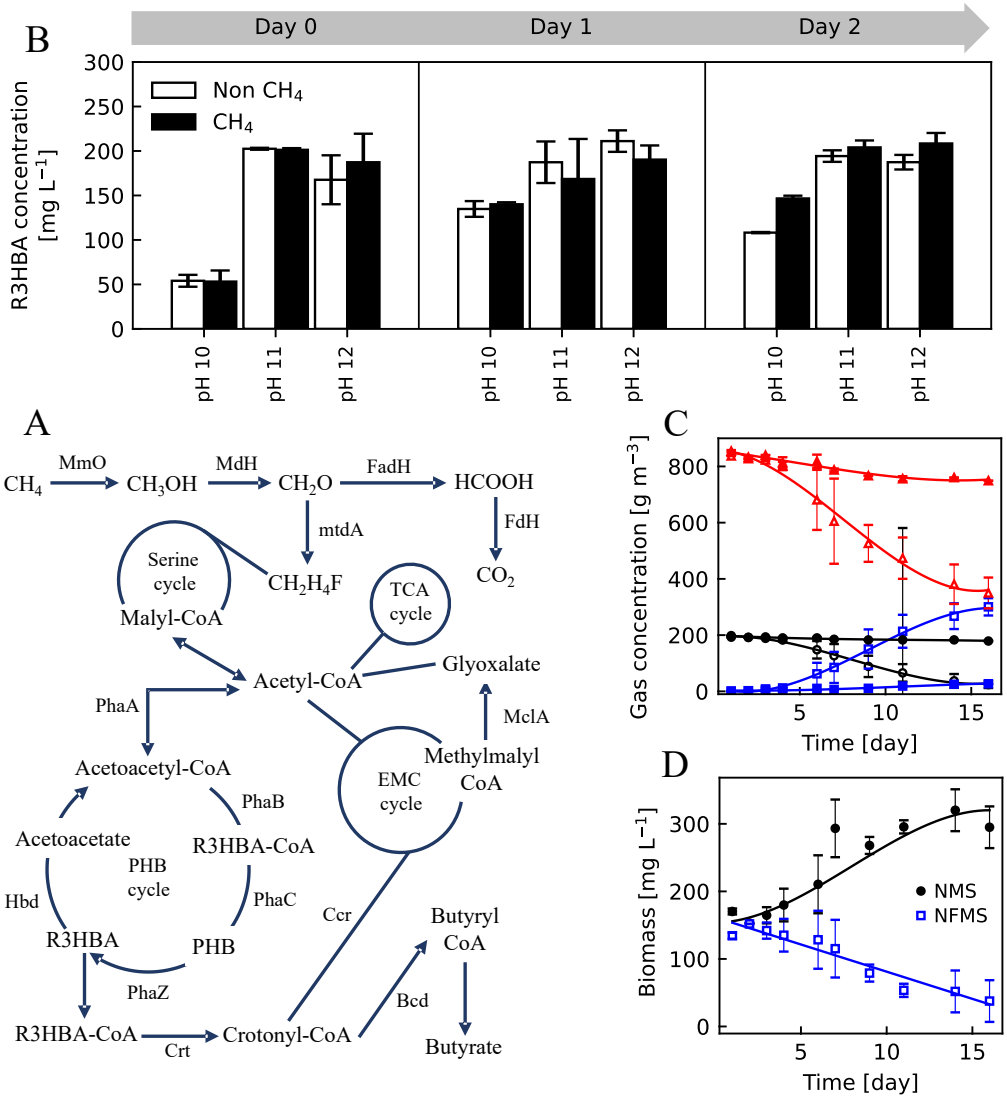

Fig. 2. Schematic representation of the metabolic pathways involved in the polymerization and depolymerization of PHB in *M. parvus* OBBP. MmO, methane monooxygenase; MdH, methanol dehydrogenase; FadH, formaldehyde dehydrogenase; FdH, formate dehydrogenase; MtdA, methylene tetrahydromethanopterin dehydrogenase; PhaA, β-ketothiolase; PhaB, acetoacetyl-CoA reductase; PhaC, PHB polymerase; Hbd, (R)-3-hydroxybutyrate dehydrogenase, Crt, 3-hydroxybutyryl-CoA dehydratase; Ccr, crotonyl-CoA carboxylase/reductase; MclA, malyl-CoA lyase; Bcd, butyryl-CoA dehydrogenase (A). R3HBA concentration in *M. parvus* at pH 10, 11 and 12 in NMS with (black bars) or without (white bars) CH_4 (B). Concentrations of biomass (C) and CH_4 (circles), O_2 (triangles) and CO_2 (square) (D) during the viability assays of *M. parvus* cells previously subjected to a 3 h depolymerization phase at pH 11. Filled and empty symbols correspond to the experiments carried out in NMS and NFMS media, respectively.

PHA at pH 11 with conversions of 76% (0.356 g L^{-1}) and 21% (0.015 g L^{-1}) in 6 h, respectively (Ren et al., 2005). Similarly, *P. putida* Bet001 can depolymerize PHAs up to 98% in 0.2 Tris-HCl buffer at pH 9.1 within 48 h (Anis et al., 2018). In Type II methanotrophs, the production of hydroxyacids has only been described in a genetically engineered *Methylosinus trichosporum* OB3b strain able to synthesize R4HBA from CH_4 via the TCA cycle and the overexpression phosphoenolpyruvate carboxylase (Ppc), isocitrate dehydrogenase (Icd) and 2-oxoglutarate dehydrogenase (SucAB). The highest 4-HB titer obtained was 10.5 mg/L after 6 culture days (Nguyen and Lee, 2021).

PHB synthesis and degradation in methanotrophic bacteria seem to be similar to the metabolic processes carried out by most heterotrophic PHB producers (Vecherskaya et al., 2001). However, there is a limited understanding of the mechanisms that bring about the intracellular PHB depolymerization and the formation of its monomer acids such as R3HBA and crotonic acid in Type II methanotrophs. Vecherskaya et al. (2001) demonstrated how products from the anaerobic fermentation of PHB in methanotrophs can be bioconverted in R3HBA, butyrate, acetate, succinate, and other reduced compounds. Fig. 2A shows the pathways of PHB depolymerization and formation of different metabolites in *M. parvus OBBP* based on a genome-scale metabolic model (Bordel et al., 2019) that has been recently reported. This model shows the fluxes of the PHB degradation from crotonyl-CoA to methylmalyl-CoA, which is dissociated into glyoxylate and propionyl-CoA. The glyoxylate originated from methylmalyl-CoA is incorporated into the serine cycle, and the propionyl-CoA is carboxylated into succinyl-CoA by the ethylmalonyl-CoA cycle (EMC) and then incorporated into the TCA cycle (Bordel et al., 2019). Another parallel pathway involves the enzymatic conversion of crotonyl-CoA to butyryl-CoA and finally to butyrate (Vecherskaya et al., 2001).

4. Optimization of pH during PHB depolymerization

The results shown in Fig. 1B indicate that PHB depolymerization at pH 11 in NMS was superior to that at low pHs in NFMS. However, these results do not clarify if pHs closer to 11 could result in higher R3HBA titers, if pH control could improve R3HBA yields or if methane plays a role in the depolymerization of PHB. In this context, *M. parvus* cells containing 18.1% of PHB were resuspended in NMS medium at 1.32 ± 0.02 gTSS $L^{-1}$and depolymerization was assessed at pHs of 10, 11 and 12 as above described. Unlike previous experiments, the pH of the cultivation broth was periodically monitored and controlled with NaOH during the course of the depolymerization.

M. parvus cells rapidly released R3HBA in the pH range of 10–12 following pH adjustment. Thus, the final extracellular monomer concentration reached 146.6 ± 3.11 mg L^{-1} and 108.2 ± 0.66 mg L^{-1} with or without methane at pH 10 (Fig. 2B). On the other hand, the influence of methane was negligible at pH 11 and pH 12, reaching a PHB depolymerization efficiency of 96.6 ± 2.22% and 92.9 ± 1.5%, respectively, (corresponding to 204 ± 7.8 mg L^{-1} and 208.44 ± 11.81 mg L^{-1} of R3HBA) in the presence of CH_4. Similar PHB depolymerization efficiencies of 98.2 ± 1.10% and 93.6 ± 1.33%, respectively, (corresponding to 194.3 ± 6.5 mg L^{-1} and 187.4 ± 8.2 mg L^{-1} of R3HBA) were recorded in the absence of CH_4 at the end of the experiment at pH 11 and 12, respectively. These data suggested that methane did not play a significant role on PHB depolymerization and that pHs beyond 11.0 exerted little influence on R3HBA release. Based on these results, pH 11 in NMS and in the absence of CH_4 was selected for further experiments. Under this condition, a PHB to R3HBA conversion of 68.0 ± 3.2% was calculated.

The fine-tuning of pH played a key role in R3HBA release and PHB depolymerization in other bacteria species. For instance, Ren et al. (2005) demonstrated that PHA depolymerization in *Pseudomonas* Gpo1 produced the highest titer of monomers (360 mg L^{-1} of 3-OH-C8) at an initial pH of 11, while a significantly smaller concentration of monomers (50 mg L^{-1}) was measured at pH 12. Similarly, depolymerization and R3HBA release in *Azohydromonas lata* peaked at a pH of 4.0 with a PHB to R3HBA conversion of 96% in 30 min, and decreased to 31% at a pH 5.0 (Lee et al., 1999). The production of R3HBA *in vivo* requires a concomitant high PHB depolymerization activity and a low enzymatic activity of Bdh. While intracellular depolymerases have an optimum pH range of 8–10 (Jendrossek and Handrick, 2002), Bdh activity is reported to be pH-dependent, with an activity range of 5–10 and an optimal pH range of 7.5–8.5, decreasing abruptly above pH 10 (Mountassif et al., 2010; Takanashi and Saito, 2006) In this context, this study suggests that the phaZ enzyme, responsible of the depolymerization of PHB towards R3HBA, of *M. parvus* exhibits a high activity at pH 11.

5. Influence of temperature on the kinetic of PHB depolymerization

Since the optimal temperature for both growth and PHB accumulation in *M. parvus* is 30 °C and no growth occurs at temperatures greater than 40 °C (Soni et al., 1998), the kinetics of PHB depolymerization and R3HBA released were investigated at 25 and 35 °C, and pH 11 (manually adjusted to compensate for the release of R3HBA). The R3HBA titers quantified at 25 °C and 35 °C were 240 ± 3.81 mg L^{-1} and 282 ± 20.04 mg L^{-1}, respectively, after 3 h of depolymerization in a cell suspension with an initial PHB concentration of 1.86 ± 0.006 g L^{-1}. The R3HBA production rates per mg of initial PHB were 48.6 ± 6.0 mg R3HBA $(mgPHBi)^{-1}h^{-1}$ at 25 °C and 52.7 ± 2.3 mg R3HBA $(mgPHBi)^{-1}h^{-1}$ at 35 °C, while PHB depolymerization reached 16.5% (Y_{3HBA} = 64.5%) and 24.8% (Y_{3HBA} = 50.5%) at 25 and 35 °C, respectively. These results were similar to those obtained by Lee et al. (1999) during the depolymerization of PHB accumulated in *Azohydromonas lata* at 30, 37 and 45 °C. A moderate increase in R3HBA production rate was found when the temperature increased from 30 to 37 °C, while PHB depolymerization suddenly stopped at 45 °C likely due to enzymatic denaturation. Since R3HBA production rate slightly increased with temperature, but R3HBA yields severely decreased, the following experiments were performed at 30 °C.

After 3 h at 25 °C and pH 10.8, cells were harvested and cultured in NMS (to assess cell growth) and NFMS (to assess PHB accumulation) media in the presence of CH_4 to analyze the viability of the cells post-depolymerization. Cells incubated in NMS medium started to consume methane and oxygen by day 4, being these gases fully depleted after 16 days (Fig. 2C). Biomass concentration increased from 170 mg L^{-1} to 295 mg L^{-1} (Fig. 2D). However, the specific growth rate (μ) of post-depolymerization cells was lower (0.058 h^{-1}) than the specific growth rate of 0.107 h^{-1} reported for fresh *M. parvus* cultures (Bordel et al., 2019). On the other hand, the culture incubated in NFMS medium experienced cell death during the cell viability experiment due to nitrogen limitation.

6. Influence of the initial R3HBA concentration and aeration rate on PHB depolymerization

To assess the effect of oxygen availability on PHB depolymerization in *M. parvus,* three tests with different liquid to air surface ratios were carried out at a constant pH of 11. Fig. 3A shows the kinetics of R3HBA release for the 72 h experiment and the depolymerization, crotonic acid and R3HBA yields in Fig. 3B. The final R3HBA concentration was similar regardless of the O_2 supply, while the largest differences were obtained for the R3HBA yield. Indeed, the lowest R3HBA yield (73.6 ± 4.9%) occurred under the condition restricting O_2 mass transfer (100 mL of broth in a 100 mL E-flask) while under less restrictive O_2 supply rates, R3HBA yields reached 84.3 ± 1.0% and 83.7 ± 2.8% at 50 mL/100 mL and 50 mL/250 mL filling ratios, respectively. In terms of PHB to R3HBA conversion, these values equate to 77.2 ± 0.9% and 75.1 ± 3.3%. Literature suggests that the oxygen content during the depolymerization process could influence the fate of the monomers produced in rather unpredictable manners. In this regard, the PHB accumulated with

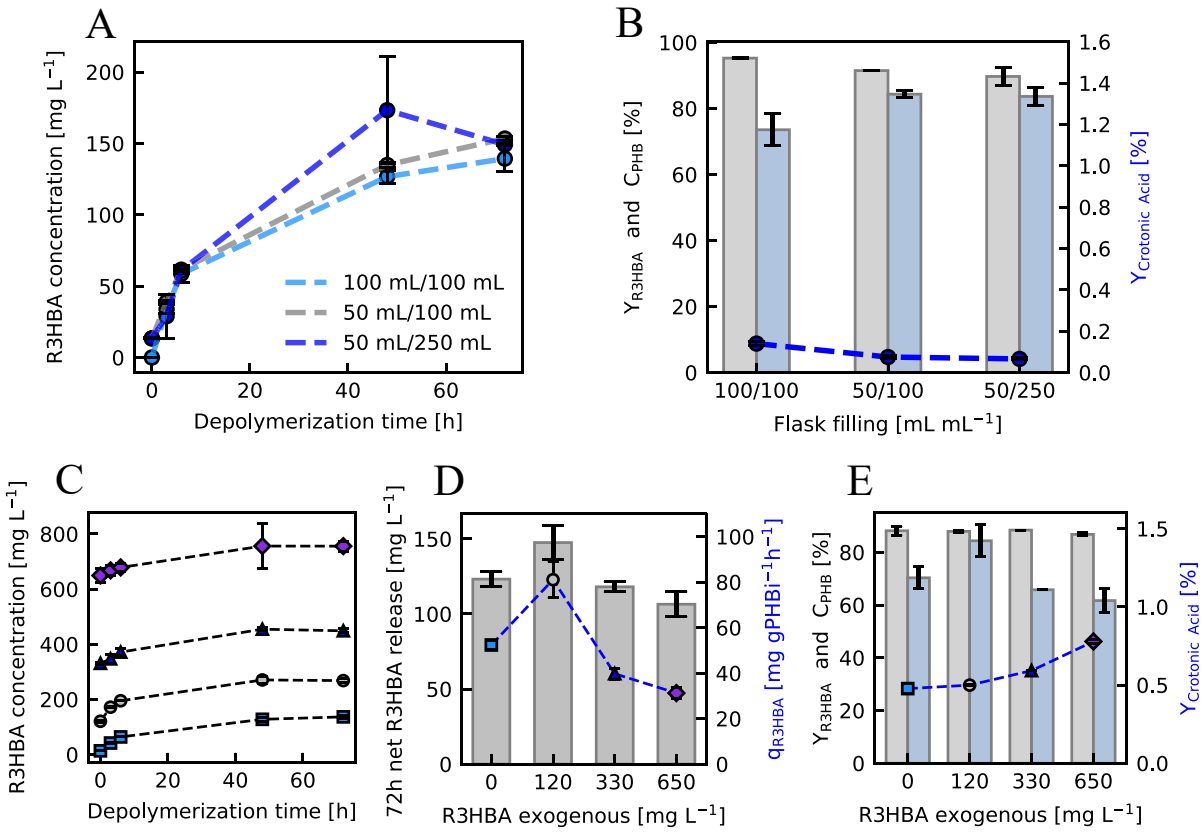

Fig. 3. Influence of the oxygen mass transfer rate on the kinetics of R3HBA excretion (A), depolymerization (grey bars) and R3HBA yields (blue bars) (B). Time course of R3HBA concentration at 0 (square), 120 (circle), 330 (triangle) and 650 (diamond) mg L^{-1} of initial R3HBA (C), net release (bars) and initial production rate of R3HBA (scatter plot) (D) and R3HBA yield (blue bars), depolymerization yield (gray bars) and crotonic acid yields (scatter plot) (E) at pH 11 and NMS medium in *M. parvus* after 72 h.

glycerol as substrate can be depolymerized to R3HBA in *Halomonas sp*. KM-1 under microaerobic conditions (25 mL of broth in 200 mL E-flasks agitated at 50 rpm) in the presence of a nitrogen source. Indeed, 15.2 g L^{-1} of R3HBA were produced in 66 h with a 76.6% PHB to R3HBA conversion under these conditions (Kawata et al., 2012). On the other hand, *Halomonas* sp. OITC1261 behaves differently despite its taxonomic closeness with *Halomonas sp*. KM-1, synthesizing R3HBA concomitantly with PHB under aerobic conditions without extra nitrogen supplementation (Yokaryo et al., 2018).

HPLC analysis of the depolymerization broth at 72 h showed that citric acid (ranging between 1 and 3 mg L^{-1} depending on the O_2 supply rate), malate (20–45 mg L^{-1}), succinate (5–20 mg L^{-1}) and crotonate (less than 0.2 mg L^{-1}) were present along with R3HBA and two unidentified compounds at 18.5 and 19.5 min in the incubation broth drawn after 72 h of depolymerization assay. In addition, a peak at 14.6 min was resolved, presumably corresponding to R3HBA dimers based on previous reports (Lu et al., 2014).

The oxygen consumption during the PHB depolymerization process at pH 11 (Fig. 1B) and the fact that the yield of R3HBA decreased as the supply of oxygen decreased below a certain threshold, suggests that part of the electrons released from the conversion of the depolymerized PHB towards acetyl-CoA are aerobically oxidized for the provision of maintenance energy. This follows from the subsequent findings: (i) the production of acetoacetate from R3HBA produces a molecule of NADH that could be used for ATP production if O_2 is available, (ii) a negligible nitrate consumption was measured at pH 11 during the depolymerization experiment, thus growth can be disregarded, (iii) a limited supply of O_2, achieved by carrying out the depolymerization process in an almost filled E-flask, decreased the R3HBA yield, suggesting that R3HBA was routed towards other metabolites to provide energy for maintenance. The latter finding can be considered as a less extreme version of the experiments by Vecherskaya et al. (2001) under anaerobic conditions, where products characteristics of a fermentative metabolism for energy production were obtained.

R3HBA, as the direct product of PHB depolymerization, might act as an inhibitor of the enzymatic depolymerization activity. To test this hypothesis in *M. parvus*, depolymerization assays were carried out adding exogenous R3HBA before the onset of the depolymerization at concentrations ranging from 0 to 650 mg L^{-1}. The higher limit was higher than the R3HBA titers achieved in previous experiments, where values slightly above 200 mg L^{-1} were found after 48 h of depolymerization at pH 11 with or without methane. Fig. 3C shows the total R3HBA concentration during the 72 h depolymerization experiment, while the net R3HBA released at the end of the experiment (72 h) is shown in Fig. 3D. No significant differences were found between R3HBA concentration released after 72 h with no added R3HBA and any of the experiments with addition of exogenous R3HBA. Fig. 3D also shows the specific initial rate of R3HBA release calculated during the first six hours. This parameter increased from 52.4 ± 1.8 mg of R3HBA per gram of initial PHB (PHBi) per hour in the absence of exogenous R3HBA to 81.1 ± 8.0 mg (g PHBi)$^{-1}$h^{-1} in the presence of 120 mg R3HBA L^{-1}. This increase could be related to impurities in the *in-house* produced R3HBA, although this was not further investigated. Additional increases in the initial R3HBA concentration led to a decrease in the specific initial rate of R3HBA release. Finally, Fig. 3E shows no differences on the depolymerization yield regardless of the initial R3HBA concentration. Interestingly, the Y_{3HBA} was reduced at 330 and 650 mg L^{-1} (65.8 ± 0 and 61.7 ± 4.40%) compared to non R3HBA addition or to 120 mg R3HBA L^{-1}

[1] added, while an increment of the crotonic acid yield to 0.78 ± 0.014% was evidenced at the highest initial R3HBA concentration.

Surprisingly, literature is scarce regarding the effect of R3HBA on the depolymerization kinetics, although R3HBA is the main reaction product. Scherer et al. (1999) found that an extracellular PHB depolymerase from *Aspergillus fumigatus* was reversibly inhibited by trimers of 3-hydroxybutyrate, but no data was presented concerning inhibition by R3HBA.

To further understand the effects of high R3HBA concentration on the depolymerization kinetics, future work will include depolymerization experiments carried out at high initial PHB concentrations. Indeed, PHB concentrations between 1 and 100 g L^{-1} could be attained by biomass concentration to test the possibility of achieving high R3HBA titers without sacrificing yield or increasing the depolymerization time.

7. Conclusion

This work showed for the first time the production of the chiral molecule (*R*)-3-hydroxybutyrate (R3HBA) from methane as a proof of concept to convert this greenhouse gas into a multicarbon value-added product. The process involves the accumulation of PHB in *Methylocystis parvus* OBBP and its in-vivo depolymerization by intracellular enzymes. A PHB to R3HBA conversion of 77.2 ± 0.9% was obtained after 72 h of depolymerization at pH 11 in a mineral medium containing nitrate under aerobic conditions. A reduced O_2 supply and increasing concentrations of exogenous R3HBA negatively affected the R3HBA yield and the initial R3HBA release rate.

CRediT authorship contribution statement

Luz Yañez: Conceptualization, Investigation, Methodology, Writing – original draft. **Yadira Rodriguez:** Conceptualization, Investigation, Methodology, Writing – original draft. **Felipe Scott:** Conceptualization, Formal analysis, Funding acquisition, Supervision, Writing – review & editing. **Alberto Vergara-Fernández:** Funding acquisition, Supervision, Writing – review & editing. **Raúl Muñoz:** Conceptualization, Funding acquisition, Project administration, Supervision, Resources, Writing – review & editing.

Declaration of Competing Interest

The authors declare that they have no known competing financial interests or personal relationships that could have appeared to influence the work reported in this paper.

Acknowledgments

This work was supported by the regional government of Castile and Leon and the EU-FEDER program (CLU 2017-09, UIC 315). The present work was also financially supported by the National Agency for Research and Development (ANID Chile), projects ANID/CONICYT Fondecyt Regular 1211434 and ANID/CONICYT Fondecyt Regular 1190521. Support from grant Apoyo a la Formación de Redes Internacionales entre Centros de Investigación REDES190137 (CONICYT-PCI) is also gratefully acknowledged.

References

Anis, S.N.S., Annuar, M.S.M., Simarani, K., 2018. Microbial biosynthesis and in vivo depolymerization of intracellular medium-chain-length poly-3-hydroxyalkanoates as potential route to platform chemicals. Biotechnol. Appl. Biochem. 65, 784–796. https://doi.org/10.1002/bab.1666.

Bordel, S., Rojas, A., Muñoz, R., 2019. Reconstruction of a Genome Scale Metabolic Model of the polyhydroxybutyrate producing methanotroph *Methylocystis parvus* OBBP. Microb. Cell Fact. 18, 1–11. https://doi.org/10.1186/s12934-019-1154-5.

Brigham, C.J., Speth, D.R., Rha, C., Sinskey, A.J., 2012. Whole-Genome Microarray and Gene Deletion Studies Reveal Regulation of the Polyhydroxyalkanoate Production Cycle by the Stringent Response in *Ralstonia eutropha* H16. Appl. Environ. Microbiol. 78, 8033–8044. https://doi.org/10.1128/AEM.01693-12.

Cao, Q., Zhang, J., Liu, H., Wu, Q., Chen, J., Chen, G.Q., 2014. The mechanism of anti-osteoporosis effects of 3-hydroxybutyrate and derivatives under simulated microgravity. Biomaterials 35, 8273–8283. https://doi.org/10.1016/j.biomaterials.2014.06.020.

Donoso, R.A., Pérez-Pantoja, D., González, B., 2011. Strict and direct transcriptional repression of the pobA gene by benzoate avoids 4-hydroxybenzoate degradation in the pollutant degrader bacterium *Cupriavidus necator* JMP134. Environ. Microbiol. 13, 1590–1600. https://doi.org/10.1111/j.1462-2920.2011.02470.x.

Edenhofer, O., 2014. IPCC 2014 Mitigation of Climate Change. Contribution of Working Group III to the Fifth Assessment Report of the Intergovernmental Panel on Climate. Cambridge University Press, Change, Cambridge.

Etminan, M., Myhre, G., Highwood, E.J., Shine, K.P., 2016. Radiative forcing of carbon dioxide, methane, and nitrous oxide: A significant revision of the methane radiative forcing. Geophys. Res. Lett. 43, 12614–12623. https://doi.org/10.1002/2016GL071930.

Fruggo. Last accessed: January 28,2022. https://www.fruugo.co.uk/contact 2021.

Irving, S.E., Choudhury, N.R., Corrigan, R.M., 2021. The stringent response and physiological roles of (pp)pGpp in bacteria. Nat. Rev. Microbiol. 19, 256–271. https://doi.org/10.1038/s41579-020-00470-y.

Jackson, R.B., Saunois, M., Bousquet, P., Canadell, J.G., Poulter, B., Stavert, A.R., Bergamaschi, P., Niwa, Y., Segers, A., Tsuruta, A., 2020. Increasing anthropogenic methane emissions arise equally from agricultural and fossil fuel sources. Environ. Res. Lett. 15 (7), 071002.

Jawaharraj, K., Shrestha, N., Chilkoor, G., Dhiman, S.S., Islam, J., Gadhamshetty, V., 2020. Valorization of methane from environmental engineering applications: A critical review. Water Res 187, 116400. https://doi.org/10.1016/j.watres.2020.116400.

Jendrossek, D., Handrick, R., 2002. Microbial degradation of polyhydroxyalkanoates. Annu. Rev. Microbiol. 56 (1), 403–432. https://doi.org/10.1146/annurev.micro.56.012302.160838.

Juengert, J.R., Borisova, M., Mayer, C., Wolz, C., Brigham, C.J., Sinskey, A.J., Jendrossek, D., Kivisaar, M., 2017. Absence of ppGpp Leads to Increased Mobilization of Intermediately Accumulated Poly(3-Hydroxybutyrate) in *Ralstonia eutropha* H16. Appl. Environ. Microbiol. 83 (13) https://doi.org/10.1128/AEM.00755-17.

Kawata, Y., Kawasaki, K., Shigeri, Y., 2012. Efficient secreted production of (*R*)-3-hydroxybutyric acid from living *Halomonas* sp. KM-1 under successive aerobic and microaerobic conditions. Appl. Microbiol. Biotechnol. 96, 913–920. https://doi.org/10.1007/s00253-012-4218-6.

Kirschke, S., Bousquet, P., Ciais, P., Saunois, M., Canadell, J.G., Dlugokencky, E.J., Bergamaschi, P., Bergmann, D., Blake, D.R., Bruhwiler, L., Cameron-Smith, P., Castaldi, S., Chevallier, F., Feng, L., Fraser, A., Heimann, M., Hodson, E.L., Houweling, S., Josse, B., Fraser, P.J., Krummel, P.B., Lamarque, J.-F., Langenfelds, R. L., Le Quéré, C., Naik, V., O'Doherty, S., Palmer, P.I., Pison, I., Plummer, D., Poulter, B., Prinn, R.G., Rigby, M., Ringeval, B., Santini, M., Schmidt, M., Shindell, D. T., Simpson, I.J., Spahni, R., Steele, L.P., Strode, S.A., Sudo, K., Szopa, S., van der Werf, G.R., Voulgarakis, A., van Weele, M., Weiss, R.F., Williams, J.E., Zeng, G., 2013. Three decades of global methane sources and sinks. Nat. Geosci. 6 (10), 813–823.

Latimer, A.A., Kakekhani, A., Kulkarni, A.R., Nørskov, J.K., 2018. Direct Methane to Methanol: The Selectivity-Conversion Limit and Design Strategies. ACS Catal. 8, 6894–6907. https://doi.org/10.1021/acscatal.8b00220.

Lee, S.Y., Lee, Y., Wang, F., 1999. Chiral compounds from bacterial polyesters: Sugars to plastics to fine chemicals. Biotechnol. Bioeng. 65, 363–368. https://doi.org/10.1002/(SICI)1097-0290(19991105)65:3<363::AID-BIT15>3.0.CO;2-1.

Liu, H., Kumar, V., Jia, L., Sarsaiya, S., Kumar, D., Juneja, A., Zhang, Z., Sindhu, R., Binod, P., Bhatia, S.K., Awasthi, M.K., 2021. Biopolymer poly-hydroxyalkanoates (PHA) production from apple industrial waste residues: A review. Chemosphere 284, 131427. https://doi.org/10.1016/j.chemosphere.2021.131427.

Lu, J., Takahashi, A., Ueda, S., 2014. 3-Hydroxybutyrate Oligomer Hydrolase and 3-Hydroxybutyrate Dehydrogenase Participate in Intracellular Polyhydroxybutyrate and Polyhydroxyvalerate Degradation in *Paracoccus denitrificans*. Appl. Environ. Microbiol. 80, 986–993. https://doi.org/10.1128/AEM.03396-13.

Matsuyama, A., Yamamoto, H., Kawada, N., Kobayashi, Y., 2001. Industrial production of (*R*)-1,3-butanediol by new biocatalysts. J. Mol. Catal. - B Enzym. 11, 513–521. https://doi.org/10.1016/S1381-1177(00)00032-1.

McAdam, B., Fournet, M.B., McDonald, P., Mojicevic, M., 2020. Production of polyhydroxybutyrate (PHB) and factors impacting its chemical and mechanical characteristics. Polymers (Basel). 12, 1–20. https://doi.org/10.3390/polym12122908.

Mountassif, D., Andreoletti, P., Cherkaoui-Malki, M., Latruffe, N., Kebbaj, M.S.E., 2010. Structural and catalytic properties of the D-3-hydroxybutyrate dehydrogenase from *Pseudomonas aeruginosa*. Curr. Microbiol. 61, 7–12. https://doi.org/10.1007/s00284-009-9568-7.

Müller-Santos, M., Koskimäki, J.J., Alves, L.P.S., de Souza, E.M., Jendrossek, D., Pirttilä, A.M., 2021. The protective role of PHB and its degradation products against stress situations in bacteria. FEMS Microbiol. Rev. 45 (3) https://doi.org/10.1093/femsre/fuaa058.

Nguyen, D.T.N., Lee, O.K., Nguyen, T.T., Lee, E.Y., 2021. Type II methanotrophs: A promising microbial cell-factory platform for bioconversion of methane to chemicals. Biotechnol. Adv. 47, 107700 https://doi.org/10.1016/j.biotechadv.2021.107700.

Nguyen, T.T., Lee, E.Y., 2021. Methane-based biosynthesis of 4-hydroxybutyrate and P (3-hydroxybutyrate-co-4-hydroxybutyrate) using engineered *Methylosinus*

trichosporium OB3b. Bioresour. Technol. 335, 125263 https://doi.org/10.1016/j.biortech.2021.125263.

Nielsen, R., Møller, N., Gormsen, L.C., Tolbod, L.P., Hansson, N.H., Sorensen, J., Harms, H.J., Frøkiær, J., Eiskjaer, H., Jespersen, N.R., Mellemkjaer, S., Lassen, T.R., Pryds, K., Bøtker, H.E., Wiggers, H., 2019. Cardiovascular Effects of Treatment With the Ketone Body 3-Hydroxybutyrate in Chronic Heart Failure Patients. Circulation 139 (18), 2129–2141. https://doi.org/10.1161/CIRCULATIONAHA.118.036459.

Pérez-Rivero, C., López-Gómez, J.P., Roy, I., 2019. A sustainable approach for the downstream processing of bacterial polyhydroxyalkanoates: State-of-the-art and latest developments. Biochem. Eng. J. 150, 107283 https://doi.org/10.1016/j.bej.2019.107283.

Pieja, A.J., Sundstrom, E.R., Criddle, C.S., 2011. Poly-3-hydroxybutyrate metabolism in the type II Methanotroph *Methylocystis parvus* OBBP. Appl. Environ. Microbiol. 77, 6012–6019. https://doi.org/10.1128/AEM.00509-11.

Ravishankara, A.R., Kulenstierna, J., Michalopoulou, E., Höglund- Isaksson, L., et al. 2021. Benefits and Costs of Mitigating Methane Emissions.

Ren, Q., Grubelnik, A., Hoerler, M., Ruth, K., Hartmann, R., Felber, H., Zinn, M., 2005. Bacterial Poly(hydroxyalkanoates) as a Source of Chiral Hydroxyalkanoic Acids. Biomacromolecules 6 (4), 2290–2298. https://doi.org/10.1021/bm050187s.

Ren, Q., Ruth, K., Thöny-Meyer, L., Zinn, M., 2007. Process engineering for production of chiral hydroxycarboxylic acids from bacterial polyhydroxyalkanoates. Macromol. Rapid Commun. 28, 2131–2136. https://doi.org/10.1002/marc.200700389.

Rodríguez, Y., Firmino, P.I.M., Arnáiz, E., Lebrero, R., Muñoz, R., 2020. Elucidating the influence of environmental factors on biogas-based polyhydroxybutyrate production by *Methylocystis hirsuta* CSC1. Sci. Total Environ. 706, 135136. https://doi.org/10.1016/j.scitotenv.2019.135136.

Rostkowski, K.H., Pfluger, A.R., Criddle, C.S., 2013. Stoichiometry and kinetics of the PHB-producing Type II methanotrophs *Methylosinus trichosporium* OB3b and Methylocystis parvus OBBP. Bioresour. Technol. 132, 71–77. https://doi.org/10.1016/j.biortech.2012.12.129.

Ruth, K., Grubelnik, A., Hartmann, R., et al., 2007. Efficient production of (*R*)-3-hydroxycarboxylic acids by biotechnological conversion of polyhydroxyalkonoates and their purification. Biomacromolecules 8, 279–286. https://doi.org/10.1021/bm060585a.

Saunois, M., Bousquet, P., Poulter, B., Peregon, A., et al., 2016. The global methane budget 2000–2012. Earth Syst. Sci. Data 8 (2), 697–751.

Scherer, T.M., Fuller, R.C., Lenz, R.W., Goodwin, S., 1999. Production, purification and activity of an extracellular depolymerase from *Aspergillus fumigatus*. J. Environ. Polym. Degrad. 7, 117–125. https://doi.org/10.1023/A:1022881204565.

Scott, F., Yañez, L., Conejeros, R., Araya, B., Vergara-Fernández, A., 2021. Two internal bottlenecks cause the overflow metabolism leading to poly(3-hydroxybutyrate) production in *Azohydromonas lata* DSM1123. J. Environ. Chem. Eng. 9 (4), 105665. https://doi.org/10.1016/j.jece.2021.105665.

Sirohi, R., Prakash Pandey, J., Kumar Gaur, V., Gnansounou, E., Sindhu, R., 2020. Critical overview of biomass feedstocks as sustainable substrates for the production of polyhydroxybutyrate (PHB). Bioresour. Technol. 311, 123536. https://doi.org/10.1016/j.biortech.2020.123536.

Soni, B.K., Conrad, J., Kelley, R.L., Srivastava, V.J., 1998. Effect of temperature and pressure on growth and methane utilization by several methanotrophic cultures. Appl. Biochem. Biotechnol. - Part A Enzym. Eng. Biotechnol. 70–72, 729–738. https://doi.org/10.1007/BF02920184.

Strong, P.J., Xie, S., Clarke, W.P., 2015. Methane as a resource: Can the methanotrophs add value? Environ. Sci. Technol. 49, 4001–4018. https://doi.org/10.1021/es504242n.

Takanashi, M., Saito, T., 2006. Characterization of two 3-hydroxybutyrate dehydrogenases in poly(3-hydroxybutyrate)-degradable bacterium, *Ralstonia pickettii* T1. J. Biosci. Bioeng. 101, 501–507. https://doi.org/10.1263/jbb.101.501.

Tieu, K., Perier, C., Caspersen, C., Teismann, P., Wu, D.-C., Yan, S.-D., Naini, A., Vila, M., Jackson-Lewis, V., Ramasamy, R., Przedborski, S., 2003. D-β-Hydroxybutyrate rescues mitochondrial respiration and mitigates features of Parkinson disease. J. Clin. Invest. 112 (6), 892–901. https://doi.org/10.1172/JCI18797.

Tokiwa, Y., Ugwu, C.U., 2007. Biotechnological production of (*R*)-3-hydroxybutyric acid monomer. J. Biotechnol. 132, 264–272. https://doi.org/10.1016/j.jbiotec.2007.03.015.

Vecherskaya, M., Dijkema, C., Stams, A.J.M., 2001. Intracellular PHB conversion in a Type II methanotroph studied by 13C NMR. J. Ind. Microbiol. Biotechnol. 26, 15–21. https://doi.org/10.1038/sj.jim.7000086.

Wang, F., Lee, S.Y., 1997. Poly(3-Hydroxybutyrate) Production with High Productivity and High Polymer Content by a Fed-Batch Culture of *Alcaligenes latus* under Nitrogen Limitation. Appl. Envir. Microbiol. 63 (9), 3703–3706. https://doi.org/10.1128/aem.63.9.3703-3706.1997.

Wendlandt, K.D., Jechorek, M., Helm, J., Stottmeister, U., 2001. Producing poly-3-hydroxybutyrate with a high molecular mass from methane. J. Biotechnol. 86, 127–133. https://doi.org/10.1016/S0168-1656(00)00408-9.

Yamanashi, T., Iwata, M., Kamiya, N., Tsunetomi, K., Kajitani, N., Wada, N., Iitsuka, T., Yamauchi, T., Miura, A., Pu, S., Shirayama, Y., Watanabe, K., Duman, R.S., Kaneko, K., 2017. Beta-hydroxybutyrate, an endogenic NLRP3 inflammasome inhibitor, attenuates stress-induced behavioral and inflammatory responses. Sci. Rep. 7 (1) https://doi.org/10.1038/s41598-017-08055-1.

Yañez, L., Conejeros, R., Vergara-Fernández, A., Scott, F., 2020. Beyond Intracellular Accumulation of Polyhydroxyalkanoates: Chiral Hydroxyalkanoic Acids and Polymer Secretion. Front. Bioeng. Biotechnol. 8 https://doi.org/10.3389/fbioe.2020.00248.

Yokaryo, H., Teruya, M., Hanashiro, R., Goda, M., Tokiwa, Y., 2018. Direct Production of (R)-3-Hydroxybutyric Acid of High Optical Purity by *Halomonas* sp. OITC1261 Under Aerobic conditions. Biotechnol. J. 13, 1–23. https://doi.org/10.1002/biot.201700343.

Zhang, J., Cao, Q., Li, S., Lu, X., Zhao, Y., Guan, J.-S., Chen, J.-C., Wu, Q., Chen, G.-Q., 2013. 3-Hydroxybutyrate methyl ester as a potential drug against Alzheimer's disease via mitochondria protection mechanism. Biomaterials 34 (30), 7552–7562. https://doi.org/10.1016/j.biomaterials.2013.06.043.